



Observation on dominance of swells over wind-seas in the coastal waters of Gulf of Mannar, India

M.M.Amrutha and V. Sanil Kumar

Ocean Engineering Division, CSIR-National Institute of Oceanography, Dona Paula, Goa 403 004 India

5

Correspondence to: Sanil Kumar (sanil@nio.org)

Abstract. In coastal gulfs generally, predominance of wind-seas are expected. Waves measured at a location having a water depth of 15 m in the nearshore waters of Gulf of Mannar during one year period (1 May 2015 to 30 April 2016) is used to examine the predominance of wind-seas and swells through spectral characterisation. The study shows that even though the location is in a gulf, the annual average value (~ 0.84 m) of the significant wave height at this area is comparable to that along the coastal waters of the Indian subcontinent, but the annual maximum value (~ 1.7 m) recorded is much less than that (3 to 5 m) observed in those regions. Also, large seasonal variations are not observed in the wave height. The waves of the study region are under the control of sea-breeze with the maximum in the late evening hours and the minimum in the early morning hours. 53% of the surface height variance in the study area is a result of southeast and south swells and the remaining are the east and southeast wind-seas.

10
15

1 Introduction

Gulf of Mannar (GoM) connects the Arabian Sea in the south to the Palk Bay in the north. Palk Bay is a shallow basin with a maximum water depth of ~ 13 m and connects to the Bay of Bengal at its northeastern end (Fig. 1). The western region of the GoM is a Marine Biosphere Reserve and slight changes in the waves and meteorological parameters will have large implications in this area. The seasonal reversal of the monsoon winds in the North Indian Ocean (Wyrtki, 1971) induces similar changes in the surface waves (Sanil Kumar et al., 2012). The winds are from the southwest in the Indian summer monsoon which lasts from June to September and from the northeast during October to January (winter monsoon). As over the rest of India, the winds in the GoM too reverse with the season (Fig. 2). Winds over the region are much stronger ($\sim 5-7$ m s^{-1}) in the summer monsoon than that ($\sim 3-5$ m s^{-1}) during the winter monsoon. Over this region, the winds during February-May is weak with a seasonal average value less than 3 m s^{-1} .

20
25

Generally, the swells propagating from distant storms and the local wind-seas represent the waves in the open ocean (Hanson and Phillips, 1999). Mixed-seas are generally observed in coastal regions, bays and gulfs with a dominance of wind-seas regime (Hwang et al., 2011). The high-frequency wave components govern the momentum flux between the ocean and atmosphere (Cavaleri et al., 2012). The long-period waves cause problems to navigation, offshore operations and



induce large motion on the moorings (McComb et al., 2009) and hence, it is necessary to know the occurrence of long-period waves at a location. Recently many studies identified long-period waves in the eastern Arabian Sea (Sanil Kumar et al., 2012; Glejin et al., 2016; Amrutha et al., 2017). Sanil Kumar et al. (2003) observed that in the Indian waters, annually the wave energy spectra are with multiple peaks for about 60% of the time and when the significant wave height (H_{m0}) is higher than 2 m, they are generally single-peaked. The multi-peaked wave spectra observed in the coastal region of India are largely dominated by swells (Sanil Kumar et al., 2003). Arena and Guedes Soares (2009) grouped the sea states with bimodal spectra in 3 sets i.e., swell dominated seas; wind-sea dominated seas and mixed-seas based on the ratio of the significant wave height of the swells and the wind-seas. When the spectrum is bimodal, the wind-seas and the swells can have different directions and it can alter the direction of the littoral drift. Gowthaman et al. (2013) observed that swells are dominant in the northern GoM from January to April and the wind-sea dominates in the remaining period of the year.

Owing to the lack of measurements, our knowledge of the wave characteristics in the western part of the GoM is poor compared to other areas. Apart from describing the seasonal variations, this study identifies the predominant wave systems in the western GoM.

2 Data and methods

Measured waves in the western GoM at a location (latitude $8^{\circ} 52' 52''$ N; longitude $78^{\circ} 17' 44''$ E) having water depth of 15 m from 1 May 2015 to 30 April 2016 are used in the study. The wave data are recorded in a moored directional waverider buoy continuously at 1.28 Hz for one year period. Heave is measured with 1 cm resolution and with 3% accuracy. The wave spectrum is estimated from the measured buoy heave data through a fast Fourier transform of 8 series, each consisting of 256 data points. The resolution of the wave spectrum is 0.005 Hz from 0.025 Hz to 0.1 Hz and thereafter it is 0.01 Hz up to 0.58 Hz. From the wave spectrum, significant wave height (H_{m0}), mean wave period (T_{m02}) and spectral peak period (T_p) are estimated for data covering 30 minutes and the wave direction is obtained based on circular moments (Kuik et al., 1988). Other parameters estimated are the maximum spectral energy density, spectral peakedness parameter (Q_p) (Goda, 1970) and spectral narrowness parameter (ν). The directional spectra are based on the Maximum Entropy Method (Lygre and Krogstad, 1986). Measurements reported in this article is in Coordinated Universal Time (UTC) and the local time is 5:30 h ahead of UTC. From the measured data, swells and wind-seas are divided through the method proposed by Portilla et al. (2009) and a separation frequency f_c is estimated. Swell and wind-sea parameters are obtained for frequency ranging from 0.025 Hz to f_c and from f_c to 0.58 Hz, respectively. The ERA-Interim (Dee et al., 2011) wind data from European Centre for Medium-Range Weather Forecasts (ECMWF) with a temporal and spatial resolution of 6-h and 0.125° is also used in the study.

The H_{m0} obtained from the third-generation spectral wave model WAVEWATCH III version 4.18 (Tolman, 1991) for the period 1 May 2015 to 30 April 2016 at 4 locations along the longitude 78.29° E is used to study the variations in the swell percentage when the waves approach from 7° N to 8.5° N. For the Southern and large part of Indian Ocean domain, the



model grid resolution is $0.5^\circ \times 0.5^\circ$ (20°E - 112°E and 70°S - 5°N) and is $0.1^\circ \times 0.1^\circ$ for the North Indian Ocean (65°E - 90°E and 5°N - 25°N). The model is forced with ERA-Interim (Dee et al., 2011) surface wind fields at every 6 h interval with a spatial resolution of 0.5° . The resolution in wave direction is at 10° and the wave frequencies are on a logarithmic scale from 0.04 to 0.5 Hz. The results of the model comparison with the measured wave data are presented in Amrutha et al. (2017).

5 3 Result and discussions

3.1 Wave parameters statistics

Based on the maxima, mean value and standard deviation, the statistical analysis of the main wave characteristics is obtained. The directional wave parameter presented here is the mean direction corresponding to the spectral peak. The annual maximum H_{m0} measured is 1.70 m and the mean value is 0.84 m (Table 1), whereas H_{m0} less than 0.34 m did not occur over the annual period. The monthly mean H_{m0} varied from 0.7 m in November to 1.08 m in June with a standard deviation of 0.12 m. Slightly higher monthly means of H_{m0} occurred during months from May to September, when means of 0.88 to 1.08 m are observed (Table 1). The lowest values occur during months from November to April. Variation in monthly average H_{m0} in a year is small (< 0.4 m) in the study area, which is in contrast to the large variations (~ 2 m) in monthly average values observed in the eastern Arabian Sea (Sanil Kumar et al., 2014). The seasonal variations in the wave height along the Indian coast have been well characterized and show a summer-winter pattern (Sanil Kumar et al., 2012). In the study area, seasonal mean H_{m0} is 0.97, 0.75 and 0.80 m during the summer, winter and fair-weather period (February-May) indicating that large seasonal variations are not observed in H_{m0} . The variation in wave height follows that of the local wind speed. Only during 20% of the time in a year, H_{m0} exceeded 1 m and no maximum wave height (H_{max}) more than 2.9 m was measured at this location. The Sri Lankan land mass is at a distance of 170 km in the north-east direction and 185 km in the south-east direction from the wave buoy location. In the N-NE direction, the Rameshwaram Island is present at a distance of 110 km. The study area is exposed to the Indian Ocean swells from south and south-west. Hence, the wave field at the study location is partially restricted and high waves are not observed compared to that in the open sea conditions along the western Bay of Bengal and the eastern Arabian Sea. Even though the study location is in a Gulf and high waves are not observed, the annual mean H_{m0} observed at the study region (0.84 m) is comparable to the values (0.7 to 1.1 m) reported for other locations in the western Bay of Bengal and eastern Arabian Sea (Gowthaman et al., 2013; Sanil Kumar et al., 2013).

On 8 November 2015, a depression was formed in the Bay of Bengal and later it was upgraded to a deep depression and crossed the coast of Tamil Nadu near Puducherry with peak wind speeds of 15.3 m s^{-1} (55 km h^{-1}) and a minimum central pressure of 991 hPa (IMD, 2015). Even though the wave measurement location is only 370 km from the track of the depression, the influence of this deep depression is not observed in the measured wave data. This shows that the waves in GoM are not influenced by the storms north of Palk Bay. Gradual increase in wave height seen in May and June is associated with the summer monsoon (Fig. 3). The locally generated waves (wind-sea) and the swells are separated to identify different wave components at the study location. Swell H_{m0} up to 1.23 m are recorded with a mean value of 0.58 m, whereas the mean



wind-sea H_{m0} is 0.56 m with a maximum value of 1.62 m. The high wind-sea H_{m0} is observed in May with negligible swell (8-10%) on that occasion; the swell was not always negligible in May.

Wide range (3 to 22 s) is observed in the peak wave period with a mean value of 12 s indicating that the wave regime of the study area consists of short to long period waves. Even though wind-seas and swells are present in the study area, the variation over an annual cycle in mean wave period is 3 to 11 s with the mean value of 4.7 s. For all months, the mean wave periods are still short relative to other areas in the western part of the Bay of Bengal and the eastern part of the Arabian Sea (5 to 6.5 s). Distribution of mean wave direction for the 3 seasons shows that the distribution is similar for the swells throughout the year except in the southwest monsoon months. However, for the wind-seas large variation in wave direction is observed from October to May. Short-period waves ($T_p < 6$ s) approach from east, northeast, southeast and south except in the southwest monsoon months. In the southwest monsoon period, the short-period waves are from southeast and south. Waves with period more than 8 s are mainly from south and southeast (Fig. 4). Over an annual cycle, 31.6% of the time, long-period waves ($T_p > 14$ s) are also observed (Table 2) and these swell waves are produced from storms in the Southern Ocean and reach the Indian coast within 5 to 6 days (Amrutha et al., 2017).

Fifty three percentage of the wave height at the study area over the annual cycle is a result of the south and southeast swells and the balance are the east and southeast wind-seas (Table 1). The wave field at the study region shows the dominance of swells over the wind-seas, which is in agreement with that reported for the areas around the Indian coast (Sanil Kumar et al., 2003; Sanil Kumar et al., 2012; Glejin et al., 2013; Sanil Kumar et al., 2014). But in the southwest monsoon period, the seasonal average swell contribution is 61%, whereas it varies from 70 to 79% for locations around India (Sanil Kumar et al., 2014).

Wind and wave direction differ by 20 to 120° during most of the time since the measurements are made close (~12 km) to the coast and the wave direction will be mostly aligned to the depth contour due to refraction, whereas such changes in wind direction are not expected (Fig. 2). Over the western GoM during most of the time, the wave climate is characterized by sea-land breeze structure and is feeble during November and December (Fig. 5). The waves in the western GoM is under the control of wind-sea generated by sea-breeze in a diurnal pattern with the maximum during the late evening and the minimum during the early morning and is similar to that reported over the south-western BoB (Glejin et al., 2013).

Wave length linked with the mean wave period ranged from 14 to 107 m and the ratio of water depth and wave length (varied from 0.11 to 0.85) is more than 0.5 during 27% of the time indicating that for 27% of the time the measured waves are in the deep water condition (USACE, 1984). On separating the waves into wind-sea and swells, it is observed that 97% of the wind-sea are in the deep water condition, whereas 98% of the time, the swells satisfies the transitional water condition. The water depth to wave length ratio shows that the wave height and the wave direction presented in this article will be influenced by the sea bed.

The wind is predominantly southwesterly from March to September and from northeast during October to February and the average wind speed is 4.8 m s⁻¹ (Figs. 3c and 4e). The nature of sea state can be recognized based on the wave age (C/U_{10}) and the steepness of wave (H_{m0}/L), where C is the phase speed corresponding to the mean wave period. Based on



wave steepness, Thompson et al. (1984) grouped ocean waves as locally generated waves, if the steepness values are greater than 0.025. The wave measurements in this study show that 61% of the time wave steepness is greater than 0.025. An old sea is defined when wave age > 25 and when the wave age < 10 , it is a young sea. For the present data, wave age is less than 10 during 98% of the time indicating young-seas with the presence of young-swells. Donelan et al. (1993) identified that the value of the spectrum at full development corresponds to $U_{10}/C_p = 0.83$, where the spectral components above this value are classified as wind-seas and that below as swells and C_p is the phase speed of the waves corresponding to the spectral peak. For the study location, the inverse wave age is more than 0.83 for 7% of the time (Fig. 6). Inverse wave age values are biased towards lower values with peaks in the range of 0.4–0.8, indicating a young-swell driven wave regime along the study area.

We have examined the variations in swell and wind-sea as the wave propagate from deep water to the shallow waters based on wave model results. The monthly average swell and wind-sea percentage along a longitude transect of 78.29° E at 7° , 7.5° , 8° and 8.5° N latitude is presented in Figure 7. The study shows that in all the months, the percentage of swells decreased as the waves moved from open ocean to Bay (7° to 8.5° N latitude) with an average decrease of $\sim 5\%$ in the swells.

3.2 Wave spectra

In order to have a better understanding of the wave systems in the study area, we show the characterization of waves through the analysis of each individual spectrum. The wave spectra are generally classified as exhibiting either one or two peaks (Henrique et al., 2015). The dominance of wind-sea or swell systems varied for both cases and are presented in this section. Measured data consists of single-peaked wind-sea, single-peaked swell and wind-sea or swell dominated multi-peaked spectra (Table 3). A majority of the data recorded are multi-peaked spectra (58.5% of the time) and the multi-peaked spectra are swell dominated during 45.3% of time and wind-sea dominated during 12.7% of the time. The single-peak spectra are mainly swell dominated. Sanil Kumar et al. (2014) reported that the occurrence of multi-peaked spectra along the eastern Arabian Sea varied from 37 to 54%.

The energy distribution of waves over a range of frequencies with time is studied by plotting the normalised wave spectral energy density in the time-frequency frame. Each wave spectrum is normalized by the maximum wave spectral energy density of the respective spectrum. Normalized spectral energy density plots in the time-frequency field indicate the predominance of spectral energy in frequency bands 0.06-0.09 Hz (corresponding to swells) during most of the time except from November to March during which the energy is in 0.18-0.24 Hz (corresponding to wind-seas) in most of the time (Fig. 8). The monthly average wave spectrum shows that the wave spectrum is swell dominated in all the months except in December and January during which the wind-seas dominate (Fig. 9). The peak of the swell part of the monthly averaged wave spectrum varied from 0.07 to 0.08 Hz.

Waves of different frequency have different directions. Long-period swells ($T_p > 14$ s) and the intermediate -period waves ($14 > T_p > 6$ s) are from 150 to 180° , whereas the wind-sea direction varies from southwest to northeast (Fig. 8). Waves with the period less than 4 s are from the northeast and east during November-March and from south-southwest



during the remaining period (Fig. 8). Monthly average wave spectrum has a similar direction for the region from 0.06 to 0.13 Hz in all months, whereas the average monthly direction varies significantly for regions beyond this frequency range (Fig. 9). For e.g., waves with the period less than 3 s are from the northeast during December-February, southwest during June-August and southeast during the remaining period. The monthly mean directional wave spectrum shows the spread of spectral energy in different frequencies and direction (Fig. 10). Two well separated peaks in spectral energy are observed from November to April, when the winter monsoon is active.

In order to have a better understanding of the wave systems in the study area, we show the characterization of waves through the analysis of each individual spectrum. The wave spectra are generally classified as exhibiting either one or two peaks (Henrique et al., 2015). The dominance of wind-sea or swell systems varied for both cases and are presented in this section. Measured data consists of single-peaked wind-sea, single-peaked swell and wind-sea or swell dominated multi-peaked spectra (Table 3). A majority of the data recorded are multi-peaked spectra (58.5% of the time) and the multi-peaked spectra are swell dominated during 45.3% of time and wind-sea dominated during 12.7% of the time. The single-peak spectra are mainly swell dominated. Sanil Kumar et al. (2014) reported that the occurrence of multi-peaked spectra along the eastern Arabian Sea varied from 37 to 54%.

The energy distribution of waves over a range of frequencies with time is studied by plotting the normalised wave spectral energy density in the time-frequency frame. Each wave spectrum is normalized by the maximum wave spectral energy density of the respective spectrum. Normalized spectral energy density plots in the time-frequency field indicate the predominance of spectral energy in frequency bands 0.06-0.09 Hz (corresponding to swells) during most of the time except from November to March during which the energy is in 0.18-0.24 Hz (corresponding to wind-seas) in most of the time (Fig. 8). The monthly average wave spectrum shows that the wave spectrum is swell dominated in all the months except in December and January during which the wind-seas dominate (Fig. 9). The peak of the swell part of the monthly averaged wave spectrum varied from 0.07 to 0.08 Hz.

Waves of different frequency have different directions. Long-period swells ($T_p > 14$ s) and the intermediate -period waves ($14 > T_p > 6$ s) are from 150 to 180°, whereas the wind-sea direction varies from southwest to northeast (Fig. 8). Waves with the period less than 4 s are from the northeast and east during November-March and from south-southwest during the remaining period (Fig. 8). Monthly average wave spectrum has a similar direction for the region from 0.06 to 0.13 Hz in all months, whereas the average monthly direction varies significantly for regions beyond this frequency range (Fig. 9). For e.g., waves with the period less than 3 s are from the northeast during December-February, southwest during June-August and southeast during the remaining period. The monthly mean directional wave spectrum shows the spread of spectral energy in different frequencies and direction (Fig. 10). Two well separated peaks in spectral energy are observed from November to April, when the winter monsoon is active.

The wave spectra grouped into different frequency ranges show that the peak frequency of a large number of wave spectra (~ 75%) falls between 0.06 and 0.1 Hz with an average H_{m0} of 0.82 m. The mean wave spectra for different peak frequency range shows that for all groups, double-peaked wave spectra is observed (Fig. 11). The intensity of the secondary



peak increased as the spectral peak frequency shifted from a low to a high frequency. The relative distance between the two peaks of the wave spectrum represented by the quotient between the mean wave period of the swell components and the mean period of the wind-sea part varied from 1.9 to 5.8 with a mean value of 3.6 and the larger values indicate more distance between the 2 peaks of the spectrum. During the study period, the spectral narrowness parameter (ν) has an average value of ~0.64 and is marginally higher (~ 0.7 to 0.9) when a multi-modal wave spectrum consisting of high-frequency local waves and the swells from the south Indian Ocean are present. The values of the spectral peakedness parameter ranged between 2 and 3 for high waves and most of the time, spectral peakedness parameter tends to be smaller since the spectral energy is distributed across the swell band.

10 4 Concluding remarks

One-year measured records of wave show that the waves are lower in the western Gulf of Mannar than in the eastern Arabian Sea and the variation in the wave height in different seasons is also less in the study area. 53% of the surface height variance in the study area is a result of the swells from the south and southeast and the balance is the wind-seas from east and southeast. The seasonal average swell contribution is less than that observed for other locations around India. A majority of the time multi-peaked spectra (58.5% of the time) are observed. Even though the study area is in a gulf region, the monthly mean wave spectrum is swell dominated in all the months with the exception of December and January during which the wind-seas dominate. Over an annual cycle, 31.6% of the time, long-period waves ($T_p > 14$ s) are observed. Wave age of the recorded data is less than 10 during 98% of the time signifying that the measured waves are the young sea mixed with the swells.

20

Acknowledgments

Authors thankfully acknowledge the CSIR, New Delhi for facilitating the research work and MoES, New Delhi for the support given for this research. We thank TMB Nair, A Nherakkol, Jeyakumar, INCOIS for the help. Dr. J. Mohanraj, Professor, Kamaraj College, Tuticorin provided the logistics during data collection and the deployment of the buoy. This work contributes part of the Ph.D. work of the first author. This work has NIO contribution No. ****.

25

References

- Amrutha, M.M., Sanil Kumar, V, Jesbin George: Observations of long-period waves in the nearshore waters of central west coast of India during the fall inter-monsoon period, *Ocean Engineering*, 131, 244-262, 10.1016/j.oceaneng.2017.01.014, 2017.
- 30 Arena, F., Guedes Soares, C.: Nonlinear high wave groups in bimodal sea states, *J. Waterway, Port, Coastal and Ocean Eng.*, 135, 69-79, 2009.



- Cavaleri, L., Fox-Kemper, B., Hemer, M.: Wind-waves in the coupled climate system. *Bull. Am. Meteorol. Soc.* 93, 1651–1661, 2012.
- Dee, D. P., Uppala, S. M., Simmons, A. J., Berrisford, P., Poli, P., Kobayashi, S., Andrae, U., Balmaseda, M. A., Balsamo, G., Bauer, P., Bechtold, P., Beljaars, A. C. M., van de Berg, L., Bidlot, J., Bormann, N., Delsol, C., Dragani, R., Fuentes, M., Geer, A. J., Haimberger, L., Healy, S. B., Hersbach, H., Hólm, E. V., Isaksen, I., Kållberg, P., Köhler, M., Matricardi, M., McNally, A. P., Monge-Sanz, B. M., Morcrette, J.-J., Park, B.-K., Peubey, C., de Rosnay, P., Tavolato, C., Thépaut, J.-N., and Vitart, F.: The ERA-Interim reanalysis: configuration and performance of the data assimilation system: The ERA-Interim reanalysis: Configuration and performance of the data assimilation system, *Q. J. Roy. Meteor. Soc.*, 137, 553–597, 2011.
- 10 Donelan, M., Dobsen, F., Smith, S., Anderson, R.: On the dependence of sea surface roughness on wave development. *J. Phys. Oceanogr.*, 23, 2143–2149, 1993.
- Glejin, J., Sanil Kumar, V., Amrutha, M.M., Singh, J.: Characteristics of long-period swells measured in the near shore regions of eastern Arabian Sea, *International J. Naval Architecture and Ocean Eng.*, 8, 312–319. doi: 10.1016/j.ijnaoe.2016.03.008, 2016.
- 15 Glejin, J., Sanil Kumar, V., Balakrishnan Nair, T.M.: Monsoon and cyclone induced wave climate over the near shore waters off Puduchery, south western Bay of Bengal. *Ocean Eng.*, 72, 277–286 <http://dx.doi.org/10.1016/j.oceaneng.2013.07.013>, 2013.
- Goda, Y.: Numerical experiments on wave statistics with spectral simulation, in: Report Port and Harbour Research Institute. Japan, 9, 3–57, 1970.
- 20 Gowthaman, R., Sanil Kumar V., Dwarakish, G.S., Soumya S. M., Jai Singh, Ashok Kumar, K.: Waves in Gulf of Mannar and Palk Bay around Dhanushkodi, Tamil Nadu, India, *Current Science*, 104(10), 1431–1435, 2013.
- Hanson, J., L., Phillips, O., M.: Wind sea growth and dissipation in the open ocean. *J. Phys. Oceanogr.*, 29, 1633–1648, 1999.
- Henrique, R., Babanin, A.V., Schulz, E., Hemer, M.A., Durrant, T.H.: Observation of wind-waves from a moored buoy in the Southern Ocean, *Ocean Dynamics*, 2015.
- 25 Hwang, P. A., Garcia-Nava, H., Ocampo-Torres, F. J.: Dimensionally consistent similarity relation of ocean surface friction coefficient in mixed seas, *J. Phys. Oceanogr.*, 41, 1227–1238, 2011.
- IMD.: Deep Depression over the Bay of Bengal (08–10 November 2015): A Report, Cyclone Warning Division, India Meteorological Department, New Delhi, http://www.rsmcnewdelhi.imd.gov.in/images/pdf/publications/preliminary-report/DD_08112015.pdf (accessed on 10 December 2016), 2015.
- 30 Kuik, A.J., Vledder, G., Holthuijsen, L.H.: A method for the routine analysis of pitch and roll buoy wave data. *J. Phys. Oceanogr.*, 18, 1020–1034, 1988.
- Lygre, A., Krogstad, H.E.: Maximum entropy estimation of the directional distribution in ocean wave spectra. *J. Phys. Oceanogr.*, 16(12):2052–2060, 1986.



- McComb, P., Johnson, D., and Beamsley, B.: Numerical model study to reduce swell and long wave penetration to Port Geraldton. Proceedings of the 2009 Pacific Coasts and Ports Conference, Wellington, New Zealand, 2009.
- Portilla, J., Ocampo-Torres, F. J., Monbaliu, J.: Spectral Partitioning and Identification of Wind Sea and Swell; *J. Atmos. Oceanic Technol.*, 26, 117-122, 2009.
- 5 Sanil Kumar, V., Glejin J., Dora, G.U., Sajiv, P. C., Singh, T., Pednekar, P.: Variations in near shore waves along Karnataka, west coast of India, *J. Earth Systems Science*, 121, 393-403. doi: 10.1007/s12040-012-0160-3, 2012.
- Sanil Kumar, V., Anand, N.M., Kumar, K.A., Mandal, S.: Multi peakedness and groupiness of shallow water waves along Indian coast. *J. Coastal Res.*, 19, 1052-1065, 2003.
- Sanil Kumar, V., Dubhashi, K.K., Balakrishnan Nair, T.M., Singh, J.: Wave power potential at few shallow water locations
10 around Indian coast, *Current Science*, 104(9), 1219-1224, 2013.
- Sanil Kumar, V., Shanas, P.R, Dubhashi, K.K.: Shallow water wave spectral characteristics along the eastern Arabian Sea, *Natural Hazards* 70, 377–394, DOI 10.1007/s11069-013-0815-7, 2014.
- Thompson, T.S., Nelson, A.R., Sedivy, D.G.: Wave group anatomy, Proceeding of 19th conference on Coastal engineering, American Society of Civil Engineers, 1, 661–677, 1984.
- 15 Tolman, H. L.: A third-generation model for wind waves on slowly varying, unsteady and inhomogeneous depths and currents. *J. Phys. Oceanogr.*, 21, 782–797, 1991.
- USACE: Shore Protection Manual, Department of the Army, U.S. Corps of Engineers, Washington, DC, 3-81 to 3-84, 1984.
- Wyrski, K.: Oceanographic atlas of the international Indian Ocean expedition. Washington, DC: National Science Foundation, 1971.

20



Table 1. Statistics of each month: mean value, standard deviation, maximum and minimum of significant wave height along with swell and wind-sea percentage in the measured data

Month	Mean (m)	Standard deviation (m)	Maximum (m)	Minimum (m)	No. of data	Swell (%)	Wind- sea (%)
May 2015	0.91	0.22	1.69	0.46	1488	54.3	45.7
June 2015	1.08	0.19	1.70	0.70	1439	58.0	42.0
July 2015	0.88	0.12	1.54	0.61	1488	64.5	35.5
August 2015	0.93	0.17	1.57	0.60	1488	63.9	36.1
September 2015	1.01	0.19	1.56	0.55	1438	58.8	41.2
October 2015	0.82	0.20	1.53	0.34	1488	63.3	36.7
November 2015	0.70	0.13	1.19	0.34	1439	59.8	40.2
December 2015	0.72	0.17	1.21	0.35	1488	30.7	69.3
January 2016	0.75	0.15	1.27	0.36	1484	28.9	71.1
February 2016	0.75	0.16	1.15	0.42	1389	38.0	62.0
March 2016	0.75	0.16	1.31	0.43	1488	53.6	46.4
April 2016	0.78	0.17	1.34	0.37	1440	60.1	39.9
Annual average	0.84	0.21	1.70*	0.34*	1463	52.8	47.2

*extremes



Table 2. Average wave parameters and number of data in different spectral peak frequencies

Frequency (f_p) range (Hz)	Number of data and %	H_{m0} (m)	T_{m02} (s)	Peak wave period (s)
$0.04 < f_p \leq 0.05$	139 (0.79)	0.91	4.98	20.14
$0.05 < f_p \leq 0.06$	1573 (8.96)	0.91	5.17	17.13
$0.06 < f_p \leq 0.07$	3838 (21.86)	0.85	4.97	14.71
$0.07 < f_p \leq 0.08$	4429 (25.23)	0.80	4.80	12.96
$0.08 < f_p \leq 0.10$	4921 (28.03)	0.82	4.71	11.06
$0.10 < f_p \leq 0.15$	368 (2.10)	0.80	4.50	8.69
$0.15 < f_p \leq 0.20$	477 (2.72)	1.05	4.03	5.30
$0.20 < f_p \leq 0.30$	1779 (10.13)	0.86	3.65	4.32
$0.30 < f_p \leq 0.50$	33 (0.19)	0.73	3.33	3.23



Table 3. Percentage of single-peaked and multi-peaked wave spectra in different months along with spectral peak period (wind-sea, swell or mixed)

Month	Single-peak (%)			Multi-peak (%)				
	Total	Wind-sea ($T_p < 6$)	Swell ($T_p > 8$)	Mixed (6 < $T_p < 8$)	Total	Wind-sea dominated ($T_p < 6$)	Swell dominated ($T_p > 8$)	Mixed (6 < $T_p < 8$)
May	40.2	0.8	39.4	0	59.8	9.7	45.6	4.6
June	55.8	0.1	55.7	0	44.2	1.7	42.1	0.4
July	57.8	0.0	57.8	0	42.2	1.1	41.1	0.0
August	48.3	0.0	48.3	0	51.7	3.3	48.4	0.0
September	51.3	0.1	51.2	0	48.7	5.6	43.0	0.2
October	48.0	0.1	47.9	0	52.0	4.2	46.9	0.9
November	47.0	0.0	47.0	0	53.0	3.3	49.8	0.0
December	15.0	0.5	14.4	0	85.0	34.2	50.8	0.0
January	9.5	0.5	9.0	0	90.5	31.4	59.1	0.0
February	25.1	0.3	24.8	0	74.9	27.5	47.4	0.0
March	43.3	0.0	43.3	0	56.7	21.8	34.8	0.0
April	56.5	0.1	56.5	0	43.5	8.5	35.0	0.0
Annual average	41.5	0.2	41.3	0.0	58.5	12.7	45.3	0.5

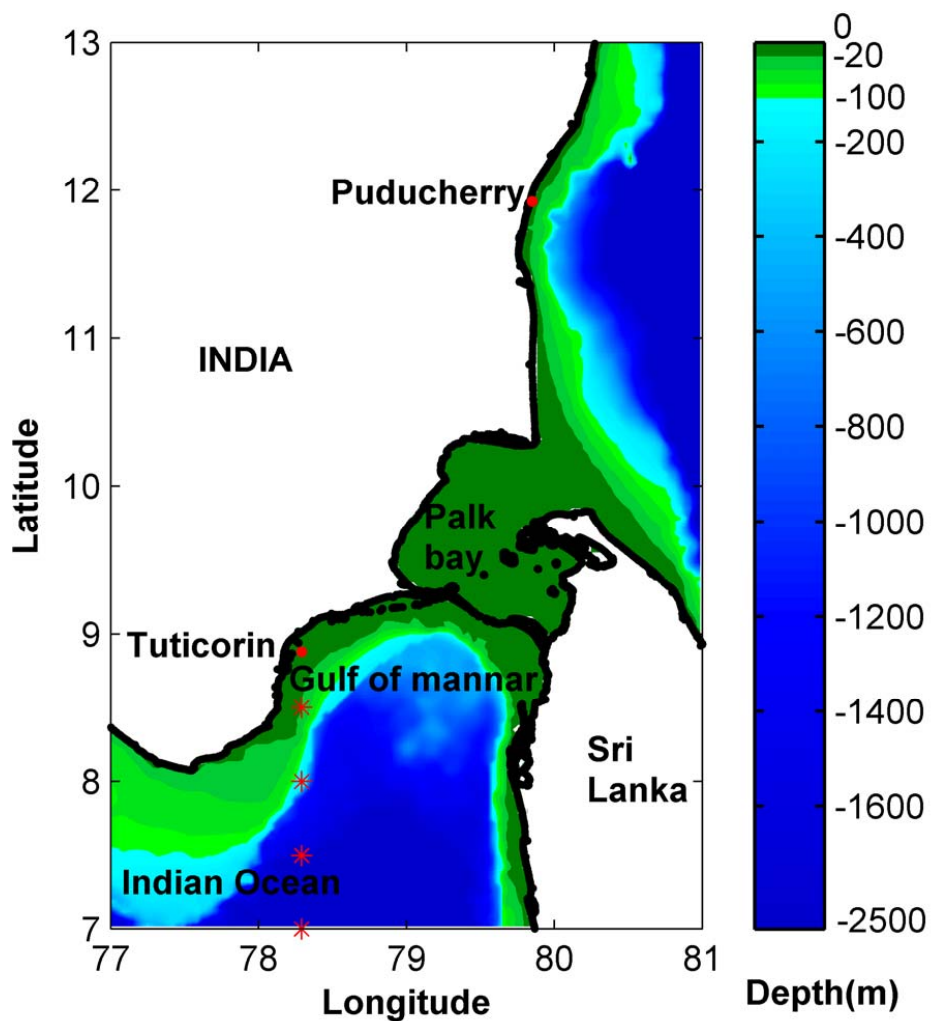


Figure 1. The location of the waverider buoy mooring in the region of interest in the Gulf of Mannar. The bathymetry is from ETOPO1, 1 Arc-Minute Global Relief Model (Amante and Eakins, 2009). The star symbol indicates the points considered for studying the percentage change in swells.

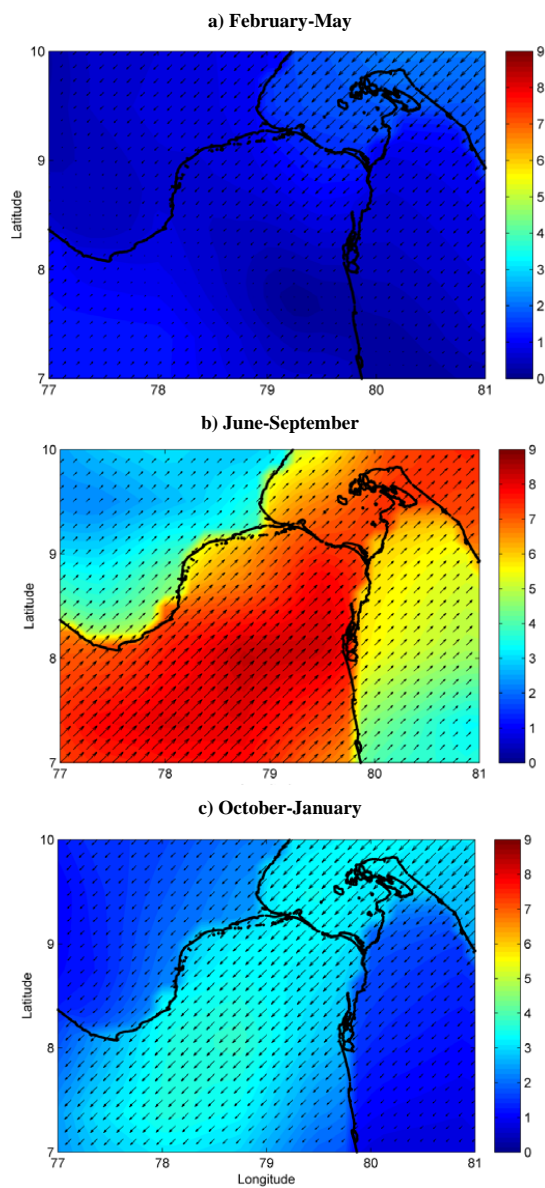


Figure 2. Wind field over the study area in different seasons; a) pre-monsoon (February-May), b) southwest monsoon (June-September) and c) northeast monsoon (October-January). Wind field is from ERA-Interim reanalysis data and the wind speed is in m s^{-1}

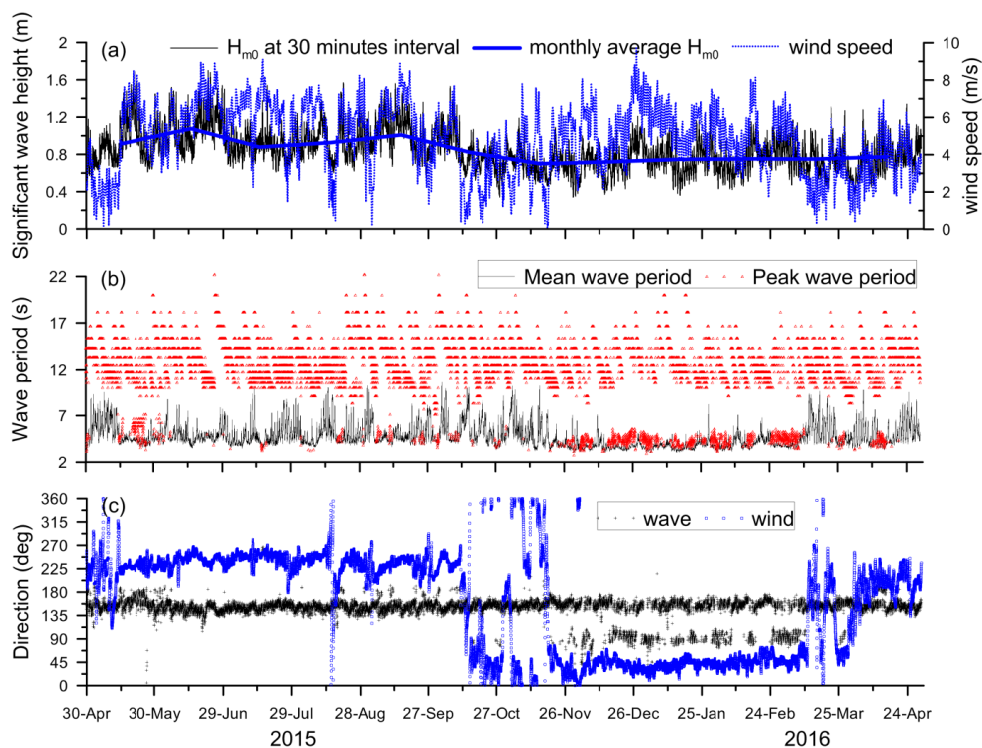


Figure 3. Time series plots of (a) significant wave height and wind speed, (b) mean wave period for data covering 30 minutes and peak wave period and (c) direction of wind and wave. The monthly average significant wave height values are also shown

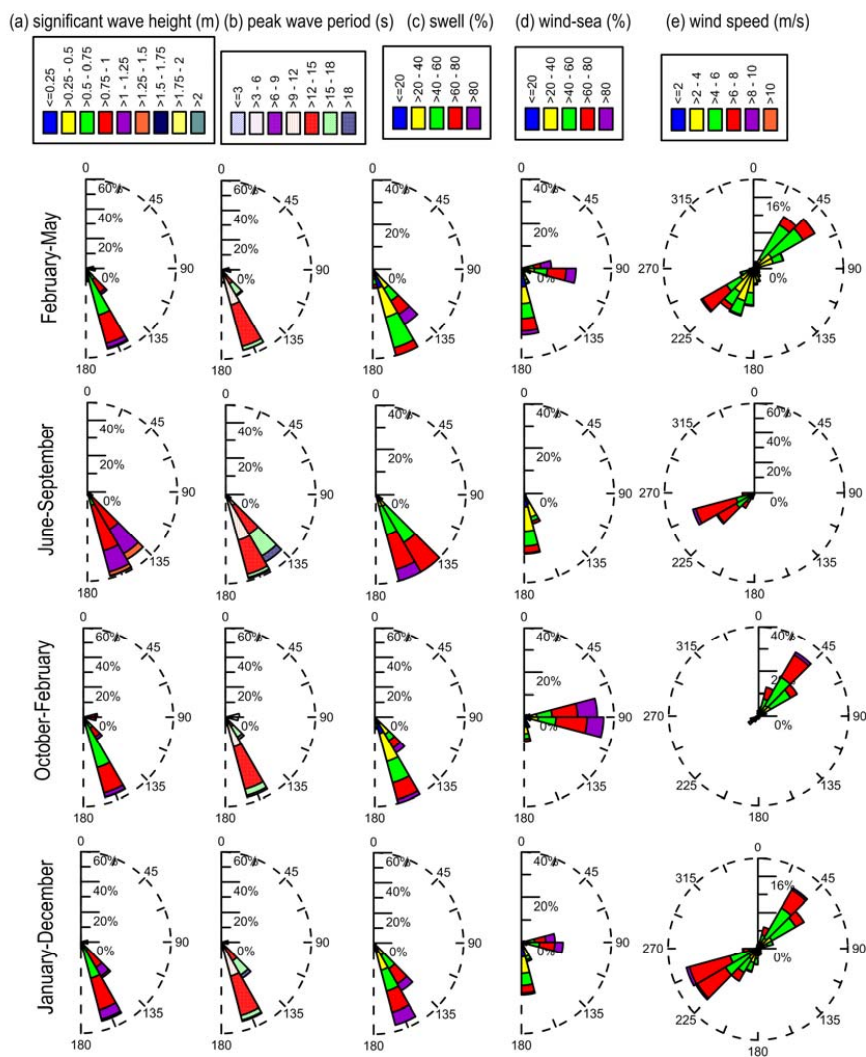


Figure 4. Wave roses during 1 May 2015 to 30 April 2016 (a) significant wave height and mean wave direction, (b) peak wave period and mean wave direction, (c) percentage of swell in the measured data and mean wave direction, (d) percentage of wind-sea in the measured data and mean wave direction, (e) wind speed and direction. The plots represent the direction where the waves come from. The radius of the figure indicates the percentage of the time.

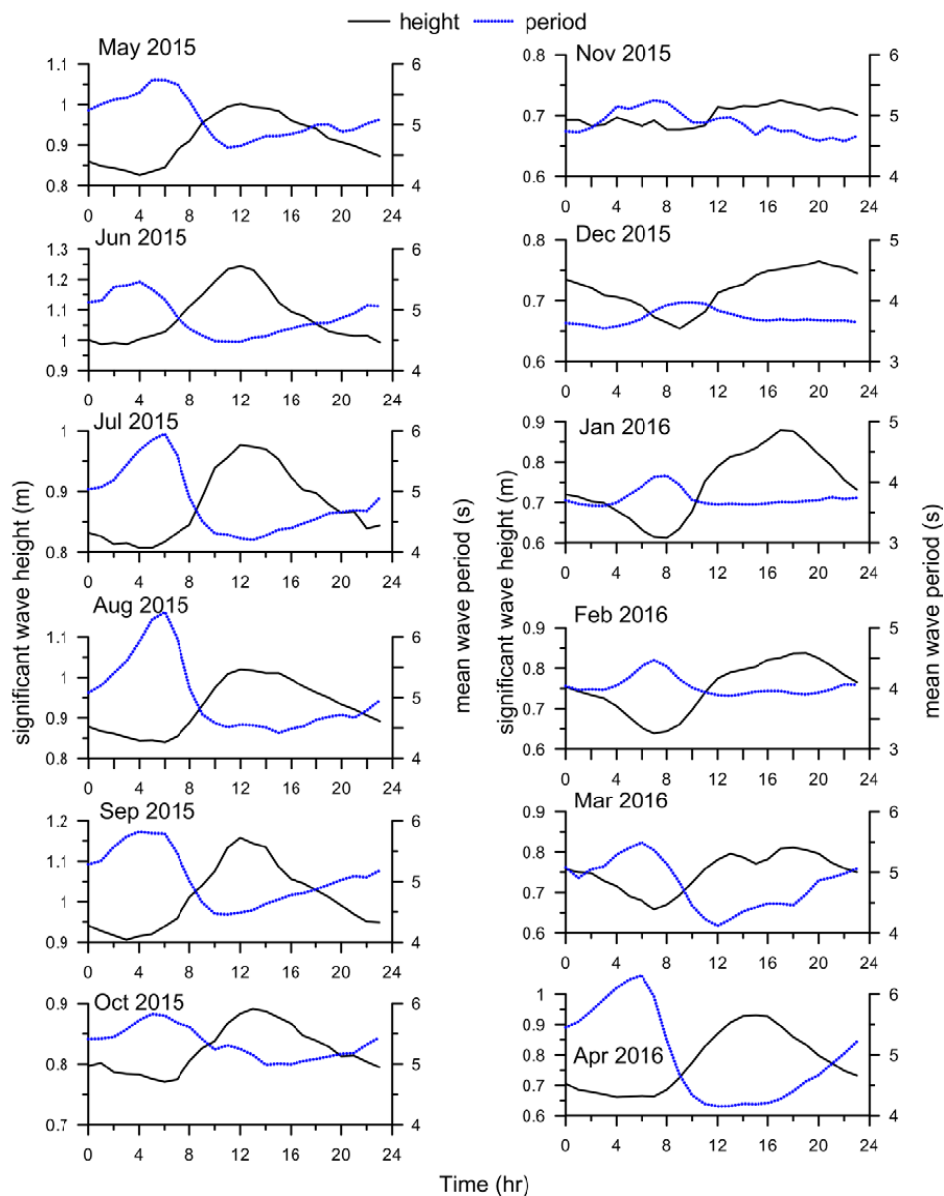


Figure 5. Variation of hourly averaged significant wave height and mean wave period in different months

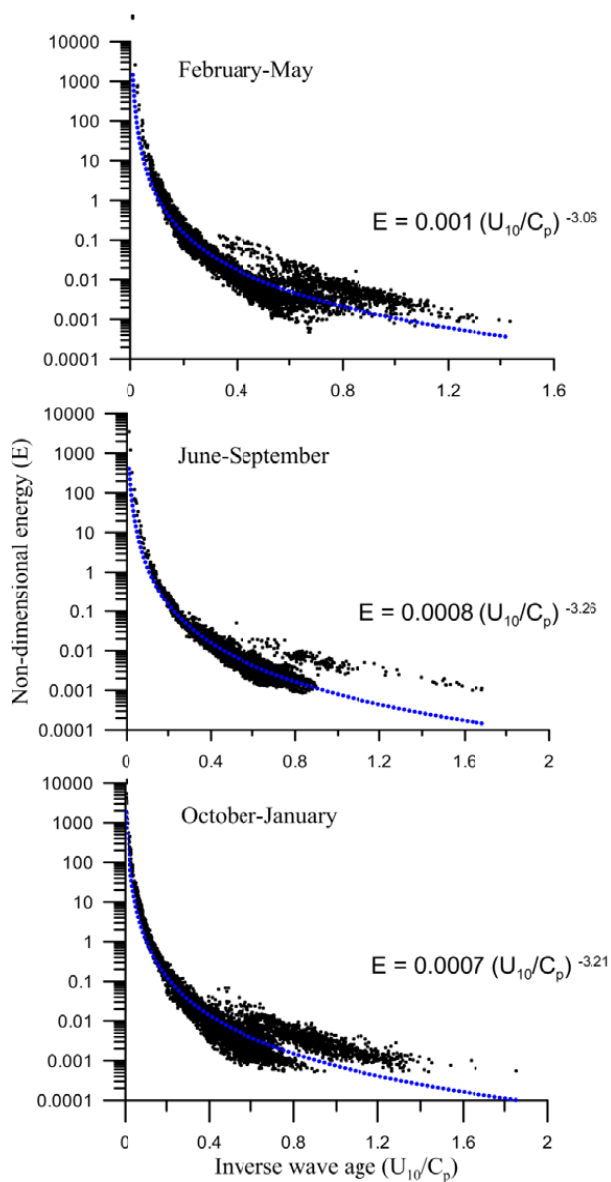


Figure 6. Variation of non-dimensional energy with inverse wave age in different periods; a) February-May, b) June-September, c) October-January

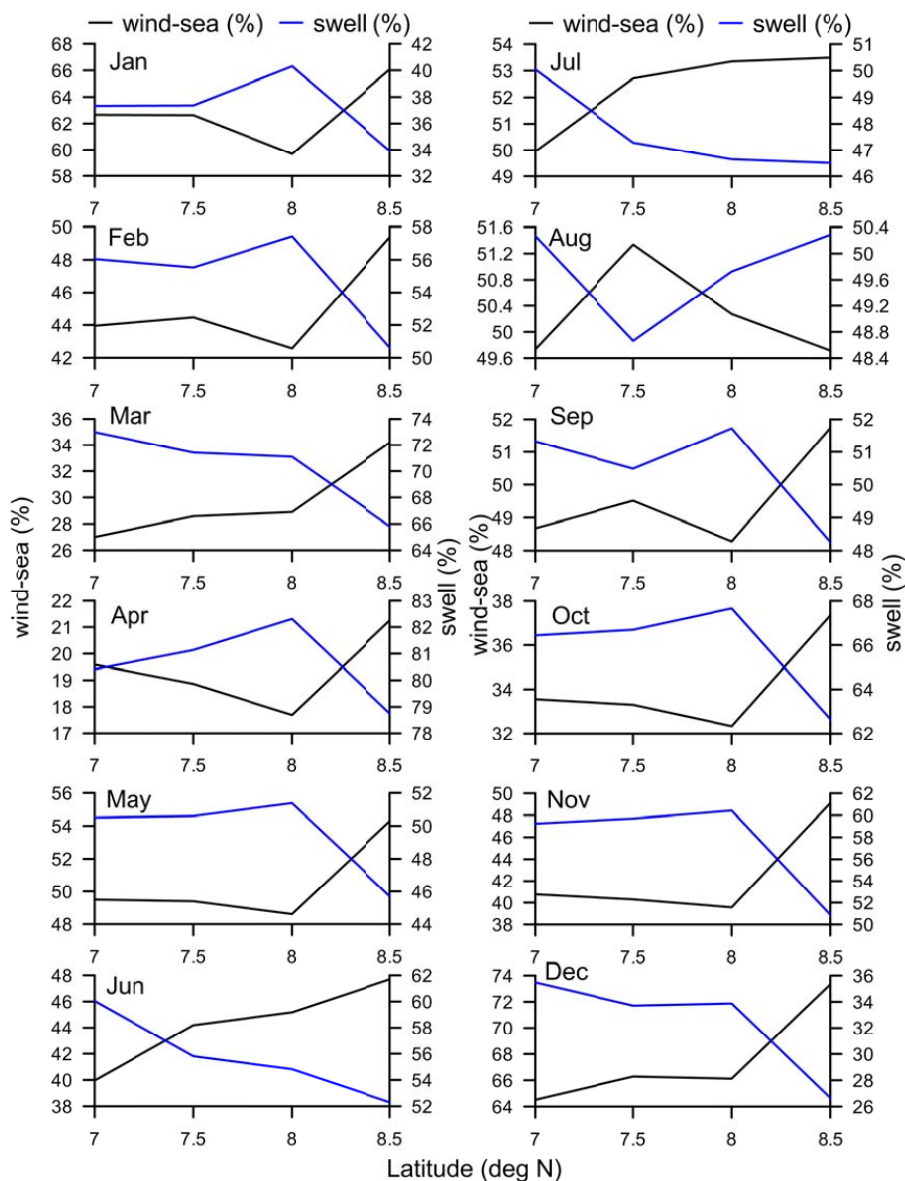


Figure 7. Swell and wind-sea percentage at 7, 7.5, 8 and 8.5° N latitude in different months based on wave model results

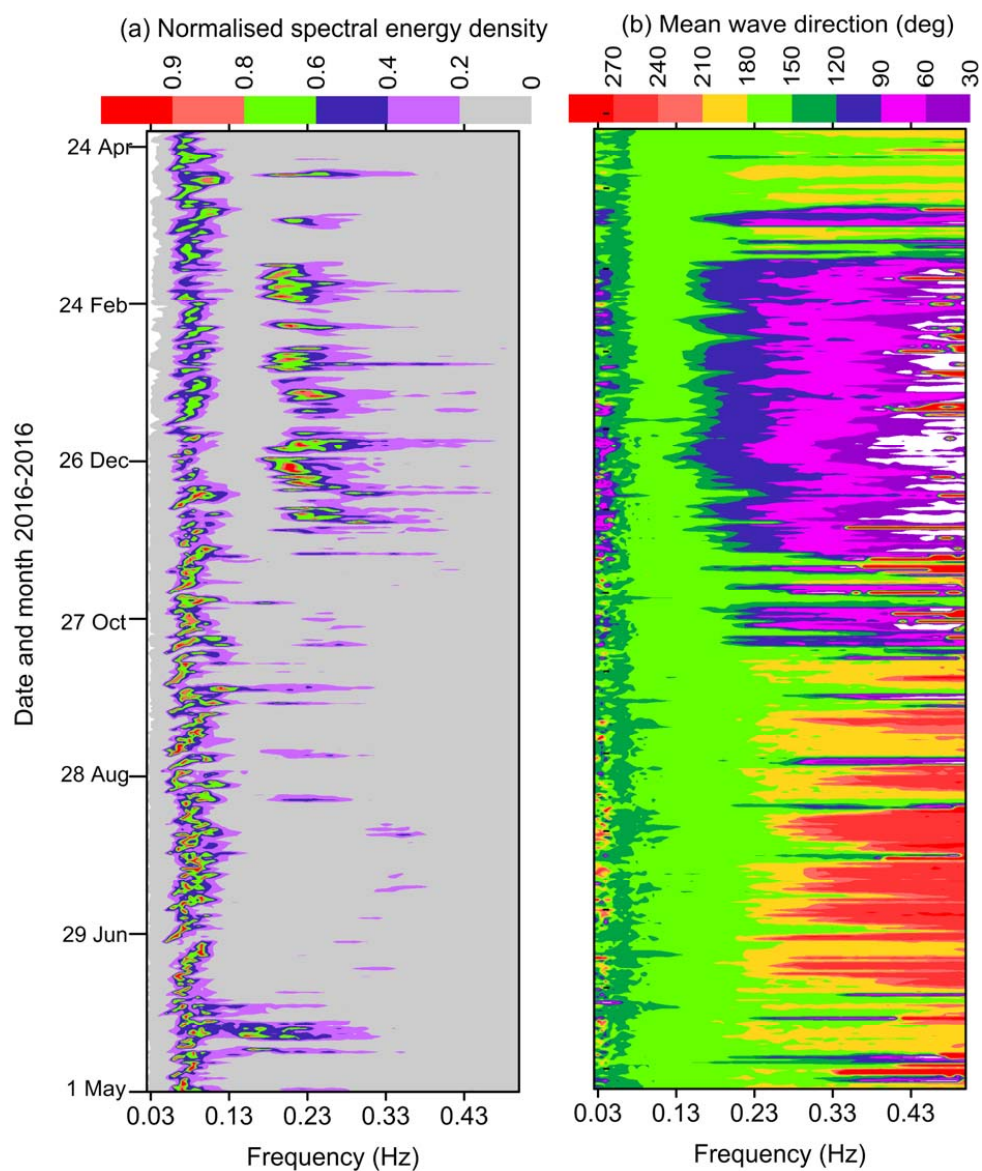


Figure 8. Contour plots of (a) normalized spectral energy density and (b) mean wave direction during 1 May 2015 to 30 April 2016

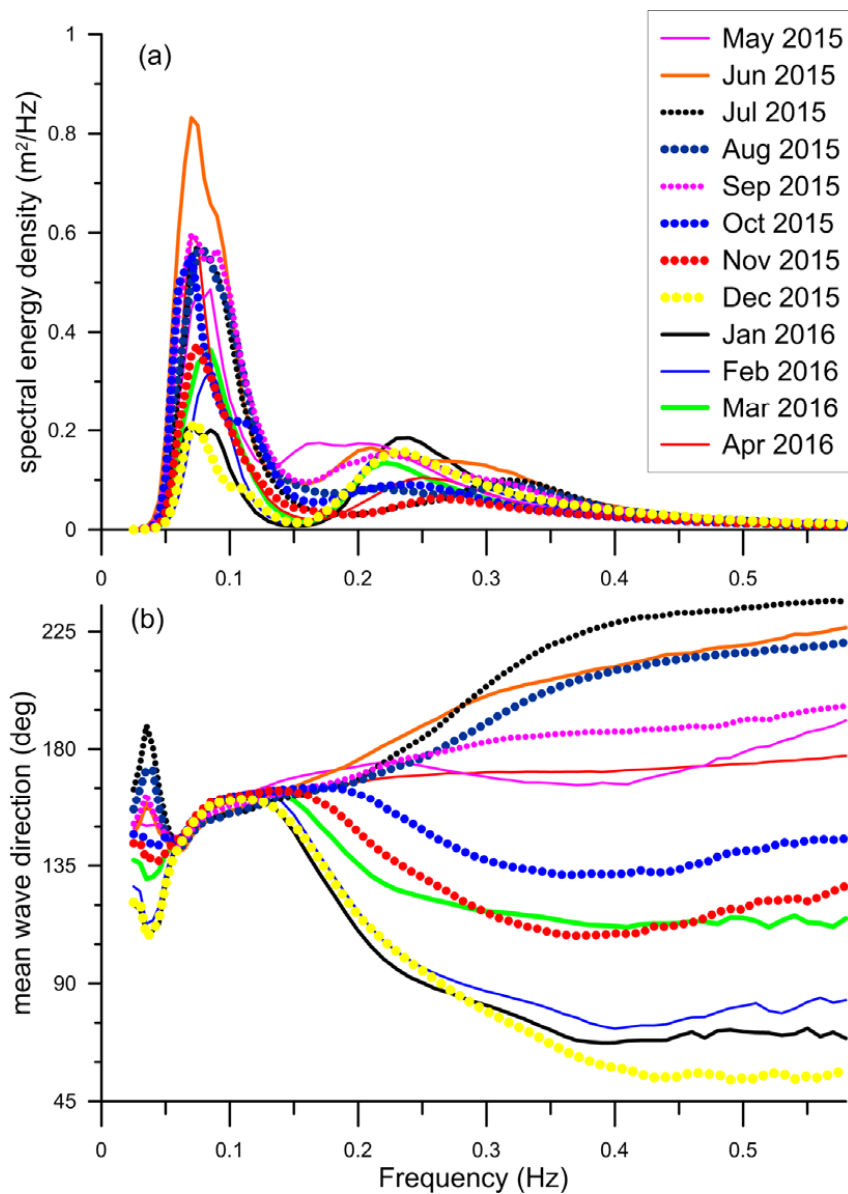


Figure 9. Monthly average wave spectrum (a) and mean wave direction (b) during May 2015 to April 2016

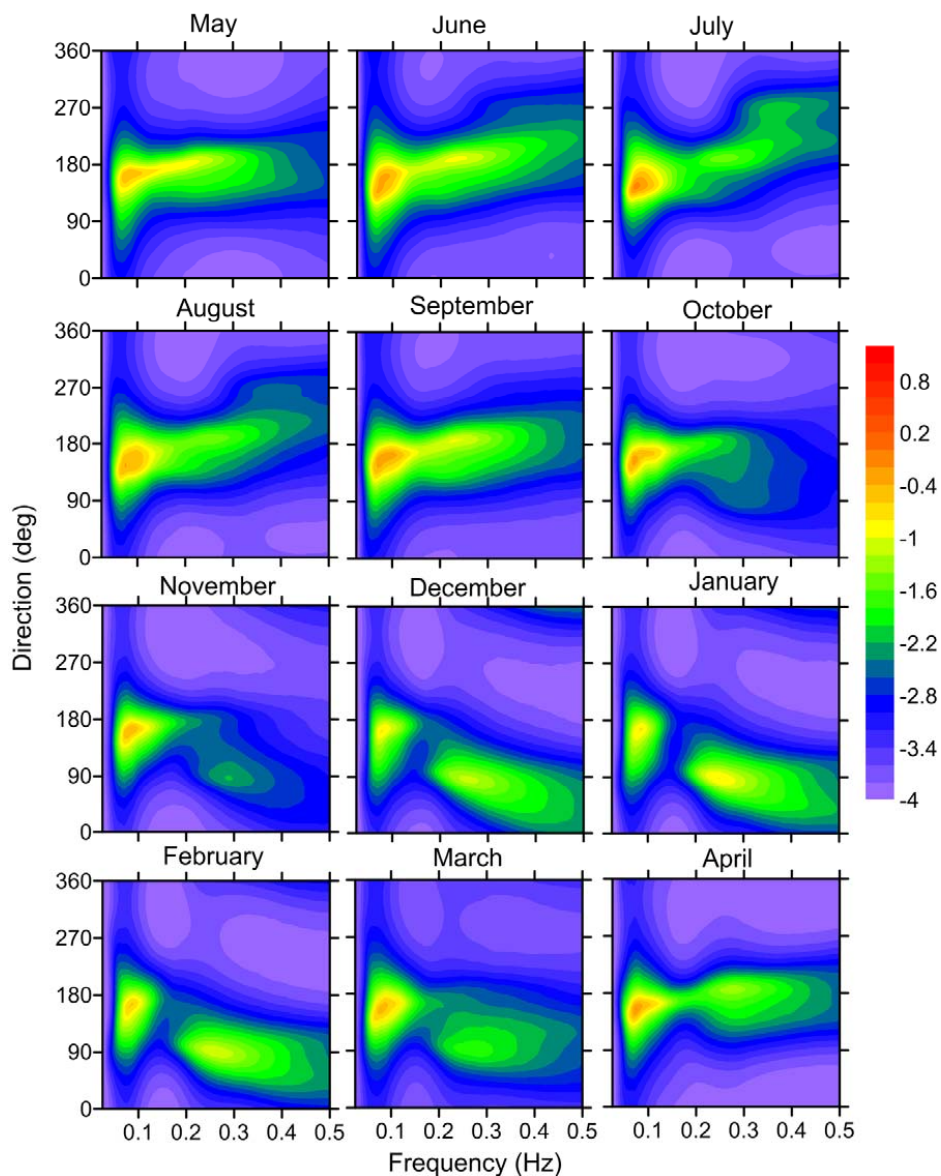


Figure 10. Monthly average directional wave spectrum during different month. The color bar is for spectral energy ($\text{m}^2 / \text{Deg}/\text{Hz}$). The spectral energy is shown in logarithmic scale (base 10).

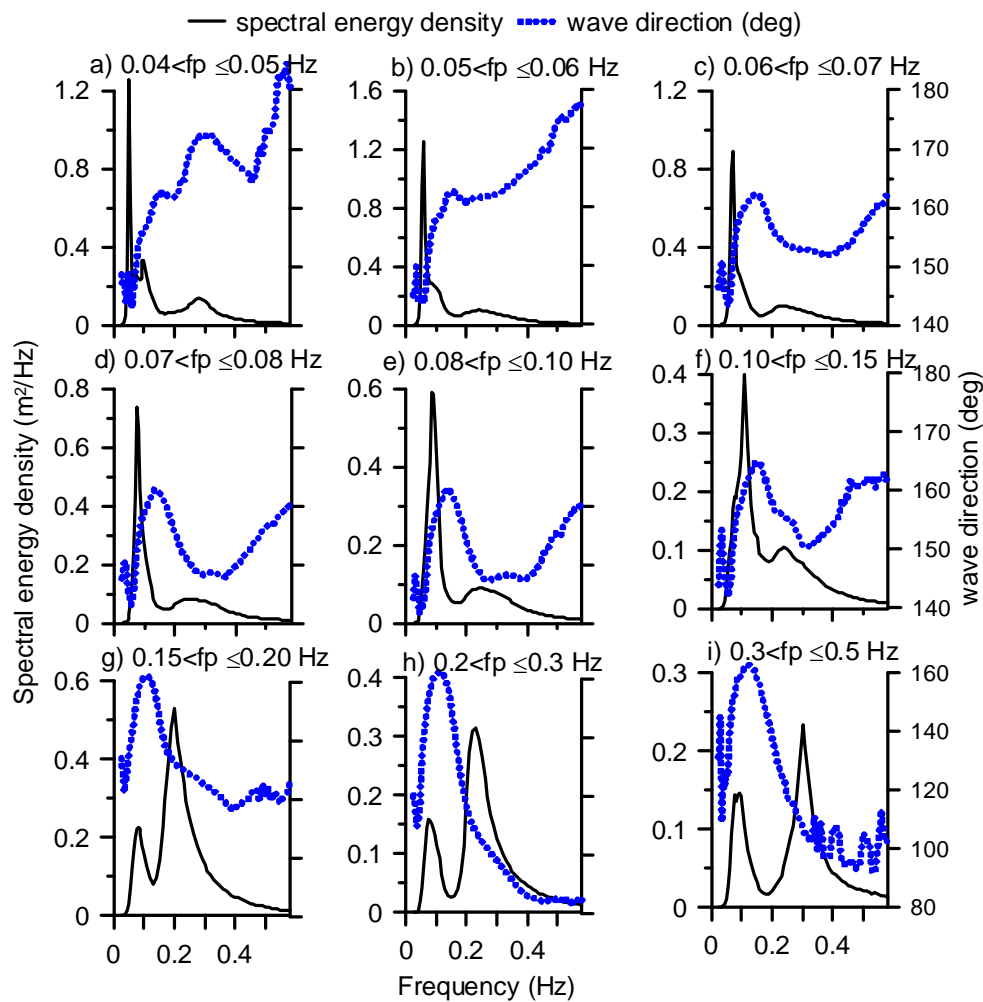


Figure 11. Plot of average spectral energy density and average mean wave direction of waves grouped under different peak frequency bins